Tuijin Jishu/Journal of Propulsion Technology
ISSN: 1001-4055
Vol. 43 No. 4 (2022)

The Effect of Chemical Reaction on an Unsteady MHD Free Convective Flow Through Porous Medium with Hall Current

[1]Ashesh Kumar Jharwal, [2]Manoj Kumar Nahlia, [3]Ajay Aaseri

[1]Assistant Professor, Department of Mathematics
Shivaji College, University of Delhi, New Delhi
[2]Assistant Professor , Department of Mathematics
Govt. Science College, Sikar, Rajasthan-332001
(P.D.S. University, Sikar, Rajasthan)
[3]Assistant Professor, Department of Mathematics
MLV Government College, Bhilwara (Rajasthan) -311001

Abstract: In this paper we investigate the effects of Chemical Reaction, Hall currents, Soret and Dufour on unsteady MHD free convective flow through porous medium in the presence of a magnetic field and first order chemical reaction. The similarity solutions were obtained using suitable transformations and the resulting similarity ordinary differential equations were solved by finite difference method. A parametric study illustrating the influence of different flow parameters on velocity, temperature and concentration fields are investigated. The skin frictions at the plate due to tangential and lateral velocity fields are obtained in non-dimensional form. The effects of the various physical parameters on these fields are discussed with help of tables and graphs.

Keywords: *MHD, porous medium, Soret number, Dufour number, hall current, porous flat plate, chemical reaction, finite difference method.*

Introduction

Combined heat and mass transfer problems with chemical reaction are of importance in many processes and have, therefore, received a considerable amount of attention in recent years. In processes such as drying, evaporation at the surface of a water body, energy transfer in a wet cooling tower and the flow in a desert cooler, heat and the mass transfer occur simultaneously. Possible applications of this type of flow can be found in many industries, For example, in the power industry, among the methods of generating electric power is one in which electrical energy is extracted directly from a moving conducting fluid. Many practical diffusive operations involve the molecular diffusion of a species in the presence of chemical reaction within or at the boundary. There are two types of reactions. A homogeneous reaction is one that occurs uniformly throughout a given phase. The species generation in a homogeneous reaction is analogous to internal source of heat generation. In contrast, a heterogeneous reaction takes place in a restricted region or within the boundary of a phase. It can therefore be treated as a boundary condition similar to the constant heat flux condition in heat transfer. The study of heat and mass transfer with chemical reaction is of great practical importance to engineers and scientists because of its almost universal occurrence in many branches of science and engineering. Jha and Srivasatava [3] have studies on effect of a chemical reaction on a moving isothermal vertical surface in presence of magnetic field with suction. Dubey et. Al [4] has studied on Effect of Chemical Reaction on MHD Free Convective Flow of Heat and Mass Transfer Past a Vertical Porous Plate with Heat Source.

Chin et al. [5] obtained numerical results for the steady mixed convection boundary layer flow over a vertical impermeable surface embedded in a porous medium when the viscosity of the fluid varies inversely as a linear function of the temperature. Gaikward et al. [6] investigated the onset of double diffusive convection in two component couple of stress fluid layer with Soret and Duffour effects using both linear and non-linear stability analysis. Hayat et al. [7] discussed the effects of Soret and Dufour on heat and mass transfer on mixed convection boundary layer flow over a stretching vertical surface in a porous medium filled with a viscoelastic fluid. Kafoussias et al.[8] considered the boundary layer flows in the presence of Soret, and Dufour effects associated with the thermal diffusion and diffusion thermo for the mixed forced natural convection. Lyubinova et al. [9] deals with the numerical investigation of the influence of static and vibrational acceleration on the measurement of diffusion and Sorect coefficients in binary mixtures, in low gravity conditions. Mansour et al. [10] investigated the effects of chemical reaction, thermal stratification, Soret and Dufour numbers on MHD free convective heat and mass transfer of viscous, incompressible and electrically conducting fluid over a vertical stretching surface embedded in a saturated porous medium.

Ming-chun et al. [11] studied Soret and Dufour effects in strongly endothermic chemical reaction system of porous media. Motsa [12] investigated the effects of Soret and Dufour numbers on the onset of double diffusive convection. Mukhopadhyay [13] performed an analysis to investigate the effects of thermal radiation on an unsteady mixed convection flow and heat transfer over a porous stretching surface in porous medium. Osalusi et al. [14] investigated thermo-diffusion and diffusion – thermo effects on combined heat and mass transfer of a steady hydro magnetic convective and slip flow due to a rotating disk in the presence of viscous dissipation and ohmic heating. Pal et al. [15] analyzed the combined effects of mixed convection with thermal radiation and chemical reaction of MHD flow of viscous and electrically conducting fluid past a vertical permeable surface embedded in a porous medium. Shateyi [16] investigated thermal radiation and buoyancy effects on heat and mass transfer over a semi-infinite stretching surface with suction and blowing. Srihari et al. [17] discussed Soret effect on unsteady MHD free convective mass transfer flow past an infinite vertical porous plate with oscillatory suction velocity and heat sink. More recently Vempati et al. [18] studied numerically the effects of Dufour and Soret numbers Fick's laws and are often neglected in heat and mass transfer processes. However, there are exceptions. The thermal-diffusion effect, for instance, has been utilized for isotope separation and in mixture between gases with very light molecular weight (Hydrogen – Helium) and of medium molecular weight (Nitrogen – Air) the diffusion thermo effect was found to be of a magnitude such that it cannot be neglected (see Kafoussias et al. [18] and reference therein).

In recent years, progress has been considerably made in the study of heat and mass transfer in magnetohydro dynamic flows due to its application in many devices. The effect of hall currents on the fluid has a lot of applications in MHD power generators, several astrophysical and meteorological studies as well as in flow of plasma through MHD power generators. From the point of applications, this effect can be taken into account within the range of magnetohydrodynamical approximation. Abreu et al. [1] examined the boundary layer solutions for the cases of forced, natural and mixed convection under a continuous set of similarity type of variables determined by a combination of pertinent variables measuring the relative importance of buoyancy force term in the momentum equation. Afify [2] carried out an analysis to study free convective heat and mass transfer of on an unsteady MHD flow past an infinite vertical porous plate with thermal radiation. Vempati et al. [18] have studies on Soret and Dufour effects on unsteady MHD flow past an infinite vertical porous plate with thermal radiation. Recently, Rao and Raju [19] have discussed on the effect of hall currents, Soret and Dufour on an unsteady MHD flow and heat transfer along a porous flat plate with mass transfer.

Motivated by the above reference work and the numerous possible industrial applications of the problem (like in isotope separation), it is of paramount interest in this study to investigate the effects of Chemical reaction, Hall currents, Soret and Dufour on unsteady MHD free convective flow through porous medium along a porous flat plate. Hence, the purpose of this paper is to extend the results of Rao and Raju [19] to study the more general problem which includes the Soret and Dufour effects on an unsteady MHD flow through porous medium and heat transfer along a porous flat plate with heat source in presence of hall currents. In this study, the effects of different flow parameters encountered in the equations are also studied. The problem is solved numerically using the finite difference method, which is more economical from the computational view point.

Mathematical Analysis

We choose $x'-$axis along the plate in the upward direction and $y'-$axis is normal to it. Initially, the temperature of the plate and the fluid through porous medium is assumed to be same. At time t' > 0, the plate starts moving with a velocity ct' in its own plane and its temperature is instantaneously raised or lowered to T which is thereafter maintained constant. Since the plate is infinite in length, all physical quantities are functions of y' and t' only. Hence, if the velocity $\overline{V}$ is given by (u', v', w'), the equation of continuity, on integration gives

$v_0' = \text{constant} = -V_0'(say)$;

Where v_0' is the constant normal velocity of suction or injection at the plate according to v_0' > 0 or < 0 respectively. Again if $\overline{H} = (H_x, H_y, H_z)$, the divergence equation of the magnetic field give H_y = constant = H_0 (say);

Where H_o is the externally applied transverse magnetic field. Using the relation $\nabla.\overline{J} = 0$ for the current density $\overline{J} = (J_x, J_y, J_z)$, we get J_y = constant.

Since the plate is non-conducting J_y = 0 at the plate and hence zero everywhere. The magnetic Reynolds number of the flow is taken to be small enough so that the induced magnetic field can be neglected. When the strength of magnetic field is very large the generalized Ohm's law in the absence of electric field takes the following form:

$$\overline{J} + \frac{\omega_e \tau_e}{B_o}\overline{J} \times \overline{H} = \sigma\left(\mu_e \overline{V} \times \overline{H} + \frac{1}{en_e}\nabla P_e\right) \quad \ldots.(1)$$

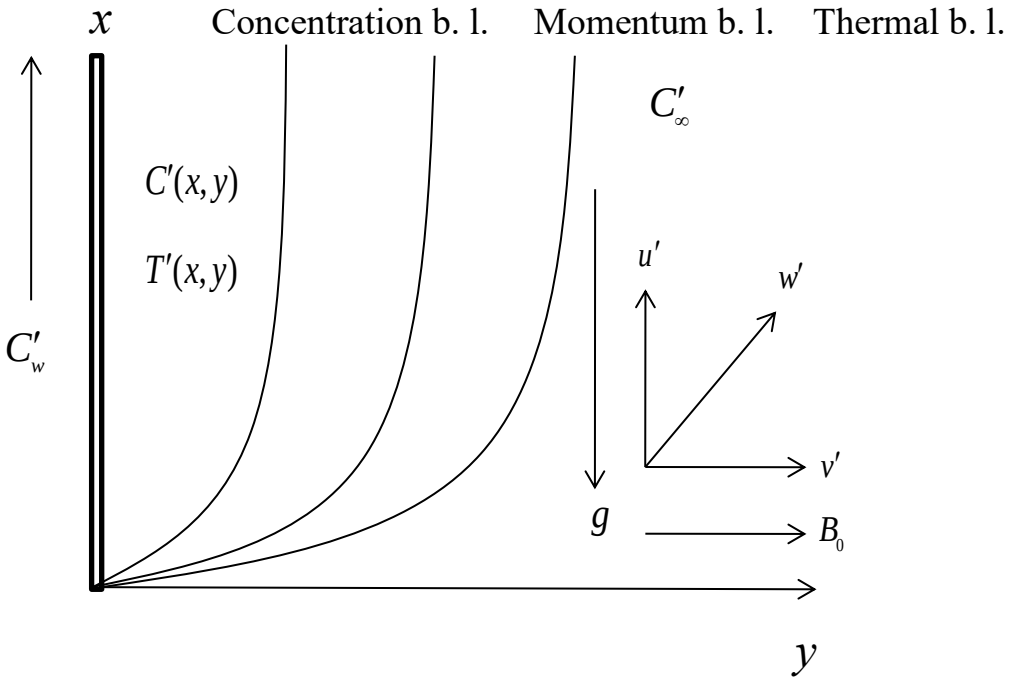

Figure 1: The coordinate system for the physical model of the problem.

Under the assumption that the electron pressure (for weakly ionized gas), the thermo-electric pressure and ion-slip are negligible, equation (1) becomes.

$$J_x = \frac{\sigma\mu_e H_o}{1+m^2}(mu' - w') \text{ and } J_z = \frac{\alpha\mu_e H_o}{1+m^2}(mw' + u') \quad \ldots.(2)$$

Where u' is the x - component of $\overline{V}$, w' is the z-component of $\overline{V}$ and m $(=\omega_e\tau_e)$ is the Hall number. Within the above framework, the equations which govern the flow under the usual Boussinesq's approximation are as follows:

$$\frac{\partial v'}{\partial y'}=0 \qquad \ldots.(3)$$

$$\frac{\partial u'}{\partial t'}+v_0'\frac{\partial u'}{\partial y'}=\upsilon\frac{\partial^2 u'}{\partial y'^2}+g\beta(T'-T_\infty')+g\beta^*(C'-C_\infty')$$

$$-\frac{\sigma\mu_e^2H_0^2}{\rho(1+m^2)}(u'+mw')-\frac{\upsilon}{K'}u' \qquad \ldots.(4)$$

$$\frac{\partial w'}{\partial t'}+v_0'\frac{\partial w'}{\partial y'}=\upsilon\frac{\partial^2 w'}{\partial y'^2}-\frac{\sigma\mu_e^2H_0^2}{\rho(1+m^2)}(w'-mu')-\frac{\upsilon}{K'}w' \qquad \ldots.(5)$$

$$\frac{\partial T'}{\partial t'}+v_0'\frac{\partial T'}{\partial y'}=\frac{k}{\rho c_p}\frac{\partial^2 T'}{\partial y'^2}+\frac{D_m k_T}{c_s\,c_p}\frac{\partial^2 C'}{\partial y'^2} \qquad \ldots.(6)$$

$$\frac{\partial C'}{\partial t'}+v_0'\frac{\partial C'}{\partial y'}=D\frac{\partial^2 C'}{\partial y'^2}+\frac{D_m k_T}{T_m}\frac{\partial^2 T'}{\partial y'^2}-K_r'(C'-C_\infty') \qquad \ldots.(7)$$

In equation (6) the term due to viscous dissipation is neglected and in equation (7) the term due to first order chemical reaction is assumed to be present. The initial and boundary conditions of the problem are:

$$\left.\begin{array}{l} t'\le 0: u'=0,\ w'=0,\ T'=T_\infty',\ C'=C_\infty' \quad for\ all\quad y' \\ t'>0: u'=Ut',\ w'=0,\ T'=T_w',\ C'=C_w' \quad at\quad y'=0 \\ \qquad u'=0,\quad w'=0,\ T'=T_\infty',\ C'=C_\infty' \quad as\quad y'\to\infty \end{array}\right\} \qquad \ldots.(8)$$

The non-dimensional quantities introduced in the equations (3) – (7) are:

$$\left.\begin{array}{l} t=t'\left(\frac{c^2}{\upsilon}\right)^{\frac{1}{3}},\quad y=y'\left(\frac{c}{\upsilon^2}\right)^{\frac{1}{3}},\quad (u,v,w)=\frac{(u',v_0',w')}{(\upsilon c)^{\frac{1}{3}}} \\ \theta=\frac{(T'-T_\infty')}{(T_w'-T_\infty')},\quad C=\frac{(C'-C_\infty')}{(C_w'-C_\infty')},\quad M=\frac{\sigma\mu_e^2H_0^2\upsilon^{\frac{1}{3}}}{\rho c^{\frac{2}{3}}} \\ Pr=\frac{\mu c_p}{k_T},\qquad Sc=\frac{\upsilon}{D},\quad Gr=\frac{\upsilon g\beta(T_w'-T_\infty')}{U^3}, \\ Gm=\frac{\upsilon g\beta^*(C_w'-C_\infty')}{U^3},\quad Du=\frac{D_m k_T(C_w'-C_\infty')}{\upsilon c_s\,c_p(T_w'-T_\infty')}, \\ Sr=\frac{D_m k_T(T_w'-T_\infty')}{\upsilon T_m(C_w'-C_\infty')},\quad K=\frac{c^{\frac{2}{3}}K'}{\upsilon^{\frac{4}{3}}},\quad K_r'=K_r\left(\frac{c^2}{\upsilon}\right)^{\frac{1}{3}} \end{array}\right\} \qquad \ldots.(9)$$

Where U is the reference velocity. The governing equations can be obtained in the dimension less form as:

$$\frac{\partial v}{\partial y}=0 \qquad \ldots(10)$$

$$\frac{\partial u}{\partial t}+v\frac{\partial u}{\partial y}=\frac{\partial^2 u}{\partial y^2}+Gr\theta+Gm\varphi-\frac{M}{(1+m^2)}(u+mw)-\frac{1}{K}u \qquad \ldots(11)$$

$$\frac{\partial w}{\partial t}+v\frac{\partial w}{\partial y}=\frac{\partial^2 w}{\partial y^2}-\frac{M}{(1+m^2)}(w-mu)-\frac{1}{K}w \qquad \ldots(12)$$

$$\frac{\partial\theta}{\partial t}+v\frac{\partial\theta}{\partial y}=\frac{1}{Pr\frac{\partial^2\theta}{\partial y^2}(Du)\left(\frac{\partial^2\varphi}{\partial y^2}\right)} \quad \ldots(13)$$

$$\frac{\partial\varphi}{\partial t}+v\frac{\partial\varphi}{\partial y}=\frac{1}{Sc}\frac{\partial^2\varphi}{\partial y^2}+(Sr)\left(\frac{\partial^2\theta}{\partial y^2}\right)-K_r\varphi \quad \ldots(14)$$

And the boundary conditions (8) in the non-dimensional form are:

$$\left.\begin{array}{l} t\le 0: u=0,\ w=0,\ \theta=0,\ \varphi=0 \quad for\ all \quad y \\ t>0: u=1, \quad w=0,\ \theta=1,\ \varphi=1 \quad at \quad y=0 \\ \qquad u=0, \quad w=0,\ \theta=0,\ \varphi=0 \quad as \quad y\to\infty \end{array}\right\} \quad \ldots(15)$$

From equation (10), we see the *v* is either constant or a function of time *t*.

Method Of Solution

The governing Equations (11) to (14) are to be solved under the initial and boundary conditions of equation (15). The finite difference method is applied to solve these equations.

The equivalent finite difference scheme of equations (11) to (14) are given by

$$\left[\frac{u_{i,j+1}-u_{i,j}}{\Delta t}\right]+v_{i,j}\left[\frac{u_{i+1,j}-u_{i,j}}{\Delta y}\right]=\left[\frac{u_{i+1,j}-2u_{i,j}+u_{i-1,j}}{(\Delta y)^2}\right]+Gr\theta_{i,j}+Gm\varphi_{i,j}$$

$$-\frac{M}{(1+m^2)}\left(u_{i,j}+mw_{i,j}\right)-\frac{1}{K}u_{i,j} \quad \ldots(16)$$

$$\left[\frac{w_{i,j+1}-w_{i,j}}{\Delta t}\right]+v_{i,j}\left[\frac{w_{i+1,j}-w_{i,j}}{\Delta y}\right]=\left[\frac{w_{i+1,j}-2w_{i,j}+w_{i-1,j}}{(\Delta y)^2}\right]$$

$$-\frac{M}{(1+m^2)}\left(w_{i,j}-mu_{i,j}\right)-\frac{1}{K}w_{i,j} \quad \ldots(17)$$

$$\left[\frac{\theta_{i,j+1}-\theta_{i,j}}{\Delta t}\right]+v_{i,j}\left[\frac{\theta_{i+1,j}-\theta_{i,j}}{\Delta y}\right]=\frac{1}{Pr\left[\frac{\theta_{i+1,j}-2\theta_{i,j}+\theta_{i-1,j}}{(\Delta y)^2}\right]}$$

$$+Du\left[\frac{\varphi_{i+1,j}-2\varphi_{i,j}+\varphi_{i-1,j}}{(\Delta y)^2}\right] \quad \ldots(18)$$

$$\left[\frac{\varphi_{i,j+1}-\varphi_{i,j}}{\Delta t}\right]+v_{i,j}\left[\frac{\varphi_{i+1,j}-\varphi_{i,j}}{\Delta y}\right]=\frac{1}{Sc}\left[\frac{\varphi_{i+1,j}-2\varphi_{i,j}+\varphi_{i-1,j}}{(\Delta y)^2}\right]$$

$$+Sr\left[\frac{\theta_{i+1,j}-2\theta_{i,j}+\theta_{i-1,j}}{(\Delta y)^2}\right]-K_r\varphi_{i,j} \quad \ldots(19)$$

Here, index *i* refers to *y* and *j* to time. The mesh system is divided by taking, $\Delta y = 0.1$.

From the boundary conditions in Equation (15), we have the following equivalent.

$$\left.\begin{array}{l} u(0,0)=0, w(0,0)=0, \theta(0,0)=0, \varphi(0,0)=0 \\ u(i,0)=0, w(i,0)=0, \theta(i,0)=0, \varphi(i,0)=0,\ for\ all\ i\ except\ i=0 \end{array}\right\} \ldots(20)$$

The boundary conditions from equation (15) are expressed in finite difference form are as follows:

$$\left.\begin{array}{l} u(0,j)=1, \quad w(0,j)=0, \quad \theta(0,j)=1, \quad \varphi(0,j)=1 \quad for\ all\ j \\ u(1,j)=0, \quad w(1,j)=0, \quad \theta(1,j)=0, \quad \varphi(1,j)=0 \quad for\ all\ j \end{array}\right\} \ldots(21)$$

Here, infinity is taken as *y* = 4.1. First, the tangential velocity of fluid at the end of time step namely $u(i, j+1),\ i=1$ to 10 is computed from equation (16), the lateral velocity of fluid at the end of time step namely $w(i, j+1),\ i=1$ to 10 is computed from equation (17) and temperature $\theta(i, j+1),\ i=1$ to 10 from equation (18) and Concentration $\phi(i, j+1), i=1$ to 10 from equation (19). The procedure is repeated until *t* = 1

(i.e., j = 800). During computation, Δt was chosen to be 0.00125. These computations are carried out for different values of parameters M, m, K, Pr, Sc, Du, Sr, K_r (Chemical Reaction parameter) and t (time). To judge the accuracy of the convergence of the finite difference scheme, the same program was run with smaller values of Δt, i.e., Δt = 0.0009, 0.001 and no significant change was observed. Hence, we conclude that the finite difference scheme is stable and convergent.

Shearing Stress

The skin – friction at the plate in the direction of tangential velocity is given by

$$\tau_1 = \left(\frac{\partial u}{\partial y}\right)_{y=0}$$

The skin – friction at the plate in the direction of lateral velocity is given by

$$\tau_2 = \left(\frac{\partial w}{\partial y}\right)_{y=0}$$

Results And Discussions

We solve the similarity equation (16), (17), (18) and (19) numerically subject to the boundary conditions given by (21). Graphical representations of the numerical results are illustrated in Figure (1) through Figure (29) to show the influences of different parameters on the boundary layer flow. In this study, we investigate the influence of the effects of material parameters such as Hartmann number (M), Hall current parameter (m), porosity parameter (K), Prandtl number (Pr), Chemical Reaction Parameter (K_r), Dufour number or diffusion Thermo (Du), Schmidt number (Sc) and Soret number or Thermal Diffusion (Sr) separately in order to clearly observe their respective effects on the tangential velocity, lateral velocity, temperature and concentration profiles of the flow. And also skin – friction coefficients (τ_1 & τ_2) have been observed through graphically. During the course of numerical calculations of the tangential velocity (u), lateral velocity (w), temperature (θ) and concentration (ϕ), the values of the Prandtl number are chosen for Air at 25°C and one atmospheric pressure (Pr = 0.71) and Water (Pr = 7.00). To focus our attention on numerical values of the results obtained in the study the values of Sc are chosen for the gases representing diffusing chemical species of most common interest in air (Sc =0.22). For the physical significance, the numerical discussions in the problem and at t = 0.5, stable values for velocity, temperature and concentration fields are obtained. To examine the effect of parameters related to the problem on the velocity field and skin – friction numerical computations are carried out at Pr = 0.71. To find solution of this problem, we have placed an infinite vertical plate in a finite length in the flow. Hence, we solve the entire problem in a finite boundary. However, in the graphs, the y values vary from 0 to 1 and the velocity, temperature and concentration tend to zero as y tend to1. This is true for any value of y. Thus, we have considered finite length.

Figures (1) – (8) display the effects of material parameters such as M, m, K, Pr, K_r, Du, Sc and Sr at Gr = 3, Gm = 3. The effect of the Hartmann number (M) is shown in figure (1). It is observed that the tangential velocity of the fluid decreases with the increase of the magnetic field number values. The decrease in the tangential velocity as the Hartmann number (M) increases is because the presence of a magnetic field in an electrically conducting fluid introduces a force called the Lorent force, which acts against the flow if the magnetic field is applied in the normal direction as in the present study. This resistive force slows down the fluid velocity component as shown in figure (1). Figure (2) depicts the tangential velocity profiles as the Hall parameter m increases. We see that u increases as m increases. It can also be observed that u profiles approach their classical values when the Hall parameter m becomes large (M > 5). Similar as the tangential velocity profiles as the porosity parameter K increases. We see that u increases as K increases in figure – (3).

Figure (4) depicts the effect of Prandtl number on tangential velocity profiles in presence of foreign species such as Air (Pr = 0.71) and water (Pr = 7.00) are shown in figure (4). We observe that from figure (4) the tangential velocity decreases with increasing of Prandtl number (Pr). The variations of tangential velocity profile for different values of chemical reaction parameter (K_r) are shown in figure (5). In this figure, we observe that as chemical reaction parameter increases, the tangential velocity of fluid decreases.

The variations of tangential velocity distribution with *y* for different values of the Dufour number (*Du*) are shown in figure (6). In this figure, it can be clearly seen that as the Dufour number increases, the tangential velocity increases.

The nature of tangential velocity profiles in presence of foreign species such as *Sc* = 0.2, 0.8 and 1.6 are shown in figure (7). The flow field suffers a decrease in tangential velocity at all points in presence of heavier diffusing species. The variations of tangential velocity distribution with *y* for different values of the Soret number (*Sr*) are shown in Figure (8). It can be clearly seen that the velocity distribution in the boundary layer increases with the Soret number. It is interesting note that the effect of Dufour and Soret numbers on velocity field are little significant. This is because either a decrease in concentration difference or an increase in temperature difference leads to an increase in the value of the Soret parameter (*Sr*). Hence increasing the Soret Parameter (*Sr*) increases the tangential velocity of the fluid.

In Figure (9), we see that lateral velocity profiles increases with the increase of the magnetic field parameter (*M*) values. The variation of lateral velocity of fluid decreases with the increase value of hall current parameter in figure (10). Figure (11) shows the variation of lateral velocity of fluid for different value of porosity parameter (*K*), It is observe that the lateral velocity increase with increases the value of porosity parameter (*K*). Figure (12) depicts the effect of Prandtl number on lateral velocity profiles in presence of foreign species such as Air (Pr = 0.71) and Pr = 1.2, 2.4 are shown in figure (12). We observe that from figure (12) the velocity is decreasing with increasing of Prandtl number (Pr). Figure (13) shows the lateral velocity profiles of boundary layer flow as the Chemical Reaction parameter K_r increases. We see that lateral velocity *w* decreases as K_r increases. The effects of Dufour parameter (*Du*) are depicted in figure (14). It is observed in this figure that the lateral velocity component increases with the increase in diffusion thermal effects. For each value of Dufour there exists a local maximum value for the lateral velocity profile. The nature of lateral velocity profiles in presence of foreign species such as *Sc* = 0.2, 0.8 and *Sc* = 0.78 are shown in figure (15). The flow field suffers a decrease in lateral velocity at all points in presence of heavier diffusing species. Figure (16) shows the effect of Soret number on the lateral velocity distribution. From this figure it can be seen that velocity component increases with the increase in Soret parameter (*Sr*). It can also be seen that at each value of *Sr* there exist local maximum values in the lateral velocity profile in the boundary region. It can be seen that as the values of this parameter increase, the lateral velocity increases.

In figure (17) we depict the effect of Prandtl number (Pr) on the temperature field. It is observed that an increase in the Prandtl number leads to decrease in the temperature field. Also, temperature field falls more rapidly for water in comparison to air and the temperature curve is exactly linear for mercury, which is more sensible towards change in temperature. From this observation it is conclude that mercury is most effective for maintaining temperature differences and can be used efficiently in the laboratory. Air can replace mercury, the effectiveness of maintaining temperature changes are much less than mercury. However, air can be better and cheap replacement for industrial purpose. This is because, either increase of kinematic viscosity or decrease of thermal conductivity leads to increase in the value of Prandtl number (Pr). Hence temperature decreases with increasing of Prandtl number (Pr). Figure (18) depicts the effects of the Dufour number on the fluid temperature. It can be clearly seen from this figure that diffusion thermal effects slightly affect the fluid temperature. As the values of the Dufour number increase, the fluid temperature also increases.

The effects of Schmidt number (*Sc*), Chemical Reaction parameter (K_r) and Soret number (*Sr*) on the concentration field are presented in figures (19), (20) and (21). Figure (19) shows that concentration field due to variation in Schmidt number (*Sc*) for the gases Hydrogen, helium, Water – vapour, Oxygen and Ammonia. It is observed that concentration field is steadily for Hydrogen and falls rapidly for oxygen and ammonia in comparison to Water – vapour. Thus Hydrogen can be used for maintaining effective concentration field and water – vapour can be used for maintaining normal concentration field. From figure (20) observe that the concentration profile of boundary layer flow decreases due to increase the Chemical reaction parameter (K_r). In figure (21), it is observed that an increase in the Soret number (*Sr*) leads to increase in the concentration field.

The profiles for skin – friction (τ_1) due to tangential velocity under the effects of Dufour number (*Du*) and Soret number (*Sr*) are presented in the table and figures (22), (23) respectively. We observe from these figures

and the above table the skin – friction (τ_1) due to tangential velocity rises under the effects of Dufour number (*Du*) and Soret number (*Sr*). The profiles for skin – friction (τ_2) due to lateal velocity under the effects of Dufour number (*Du*) and Soret number (*Sr*) are presented in the table and figures (24), (25) respectively. We see from these figures the skin – friction (τ_2) due to lateral velocity rises under the effects of Dufour number (*Du*) and Soret number (*Sr*).

M	*m*	*K*	Pr	*Sc*	K_r	*Du*	*Sr*	τ_1	τ_2
1	1	2	0.71	0.4	0.01	0.2	0.2	0.26516	0.095082
2	1	2	0.71	0.4	0.01	0.2	0.2	0.168638	0.187149
1	2	2	0.71	0.4	0.01	0.2	0.2	0.32275	0.076798
1	1	5	0.71	0.4	0.01	0.2	0.2	0.322474	0.095995
1	1	2	0.71	0.4	0.01	0.2	0.2	0.626101	0.098066
1	1	2	0.71	0.4	0.01	0.2	0.2	0.642145	0.098434
1	1	2	2.4	0.4	0.01	0.2	0.2	0.217316	0.093974
1	1	2	0.71	0.8	0.01	0.2	0.2	0.239816	0.094497
1	1	2	0.71	0.4	1	0.2	0.2	0.252134	0.095013
1	1	2	0.71	0.4	0.01	2	0.2	0.304989	0.095996
1	1	2	0.71	0.4	0.01	0.2	1.6	0.278278	0.095446

References

[1] Abreu, C.R.A., Alfradique, M.F., and Telles, A.S.,: Boundary layer flows with Dufour and Soret effects; I: forced and natural convection, Chemical Engineering Science, 61, 4282-4289(2006).

[2] Afifty, A.A., 2009. Similarity solution in MHD: Effects of thermal diffusion and diffusion thermo on free convective heat and mass transfer over a stretching surface considering suction and injection, Common. Nonlinear Sci Numer Simulat., 14, 2202-2214.

[3] Jha, Rajeev and R. K. Srivasatava, 2006. Effect of a chemical reaction on a moving isothermal vertical surface in presence of magnetic field with suction. Journal of The Aligarh Bulletin of Mathematics, Vol. 25, No. 1, Page 33- 41.

[4] Dubey, Anurag., Singh, U. R. and Rajeev Jha, 2011. Effect of Chemical Reaction on MHD Free Convective Flow of Heat and Mass Transfer past a Vertical Porous Plate with Heat Source. International Journal of stability and fluid Mechanics, Vol.2, Issue No. 2, Pages: 173-185.

[5] Chin, K.E., Nazar R., Arifin N.M., and Pop, 1., 2007. Effect of variable viscosity on mixed convection boundary layer flow over a vertical surface embedded in a porous medium. International Communications in Heat and Mass Transfer, 34, 464-473.

[6] Gaikwad, S.N., and Malashetty, M.S., and Prasad, K.R., 2007. An analytical study of linear and non-linear double diffusive convection with Soret and Dufour effects in couple stress fluid, International Journal of Non linear Mechanics, 42, 903-913.

[7] Hayat, T., Mustafa, M., and Pop, 1, 2009. Heat and mass transfer for Soret and Dufour effects on mixed convection boundary layer flow over a stretching vertical surface in a porous medium filled with a viscoelastic fluid. Communications in Nonlinear Science and Numerical Simulation, 15, 1183-1196.

[8] Kafoussias, N.G., and Williams, E.W., 1995. Thermal-diffusion and diffusion-thermo effects on mixed free forced convective and mass transfer boundary layer flow with temperature dependent viscosity, International Journal of Engineering Science, 33, 1369-1384.

[9] Lyubimova, T., Shyklyaeva, E., Legros., J.C., Shevtsova, V., and Roux, 2005. Numerical study of high frequency vibration influence on measurement of Soret and diffusion coefficients in low gravity conditions. Advances in space Research, 36, 70-74.

[10] Mansour, M.A., El-Anssary, N.F., and Aly, A.M., 2008. Effects of chemical reaction and thermal stratification on MHD free convective heat and mass transfer over a vertical stretching surface embedded in a porous media considering Soret and Dufour numbers, Journal of Chemical Engineering, 145, 340-345.

[11] Ming – chun, Li., Yan – wen, T., and Yu – chun, Z., 2006. Soret and Dufour effects in strongly endothermic chemical reaction system of porous media, Trans. Nonferrous Met. Soc. China, 16, 1200-1204.

[12] Mosta, S.S., 2008. On the onset of convection in a porous layer in the presence of Dufour and Soret effects. SAMSA Journal of Pure and Applied Mathemathics,3, 58-65.

[13] Mukhopadhyay S., 2009. Effect of thermal radiation on unsteady mixed convection flow and heat transfer over a porous stretching surface in porous medium. International Journal of Heat and Mass Transfer, 52, 3261-3265.

[14] Osalusi, E., Side. And Harris R., 2008. Thermal-diffusion and diffusion-thermo effects on combined heat and mass transfer of steady HD convective and slip flow due to a rotating disk with viscous dissipation and Ohmic heating, International Communications in Heat and Mass transfer, 35, 908 – 915.

[15] Pal. D., and Talukdar, B., 2010. Buoyancy and chemical reaction effects on MHD mixed convection heat and mass transfer in a porous medium with thermal radiation and Ohmic heating, Common Nonlinear Sci., Numer Simulate., 15, 2878-2893. DOI: 10.1016/j. cnsns. 2009.10.029

[16] Shateyi, S., 2008. Thermal radiation and buoyancy effects on heat and mass transfer over a semi infinite stretching surface with suction and blowing, Journal of Applied Mathematics, doi:10.1155/2008/414830.

[17] Srihari. K., Reddy, S.R., and Rao, J.A. 2006. Soret effect on unsteady MHD free convective mass transfer flow past an infinite vertical porous plate with oscillatory suction velocity and heat sink. International Journal of Applied Mathematical Analysis and Applications, 1, 239-259.

[18] Vempati, S.R., and Laxmi-narayana-gari. A.B., 2010. Soret and Dufour effects on unsteady MHD flow past an infinite vertical porous plate with thermal radiation. Appl. Math., Mech., - Engl. Ed., 31, 1481 – 1496. DOI: 10.100., s10483 – 010 – 1378 – 9.

[19] Rao, J. A. and Raju, R. Srinivisa, The effect of hall currents, Soret and Dufour on an unsteady MHD flow and heat transfer along a porous flat plate with mass transfer, Journal of Energy, Heat and Mass Transfer, Vol. 33, pp.351-372, (2011)

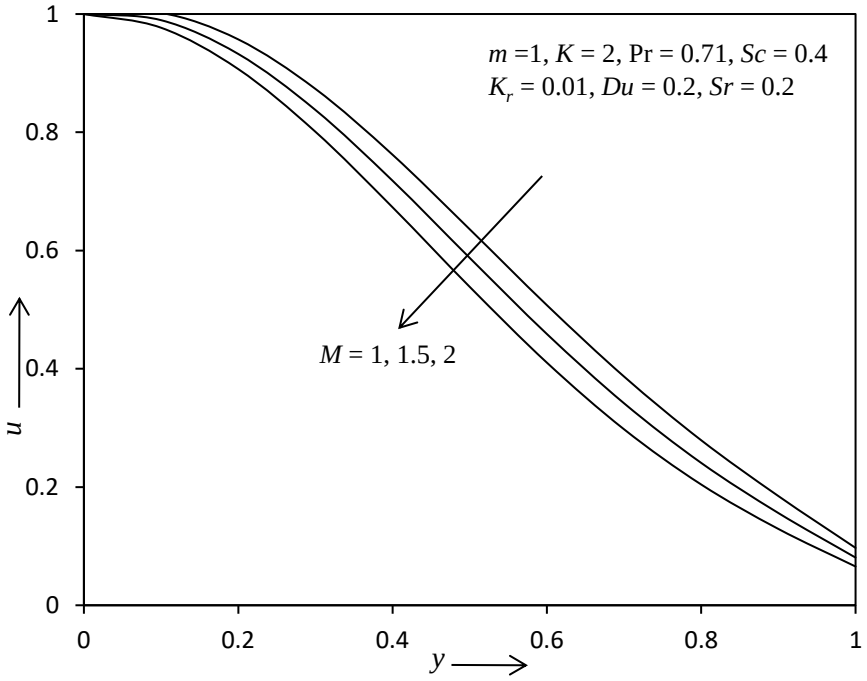

Fig. - 1: The tangential velocity profile for different value of *M*.

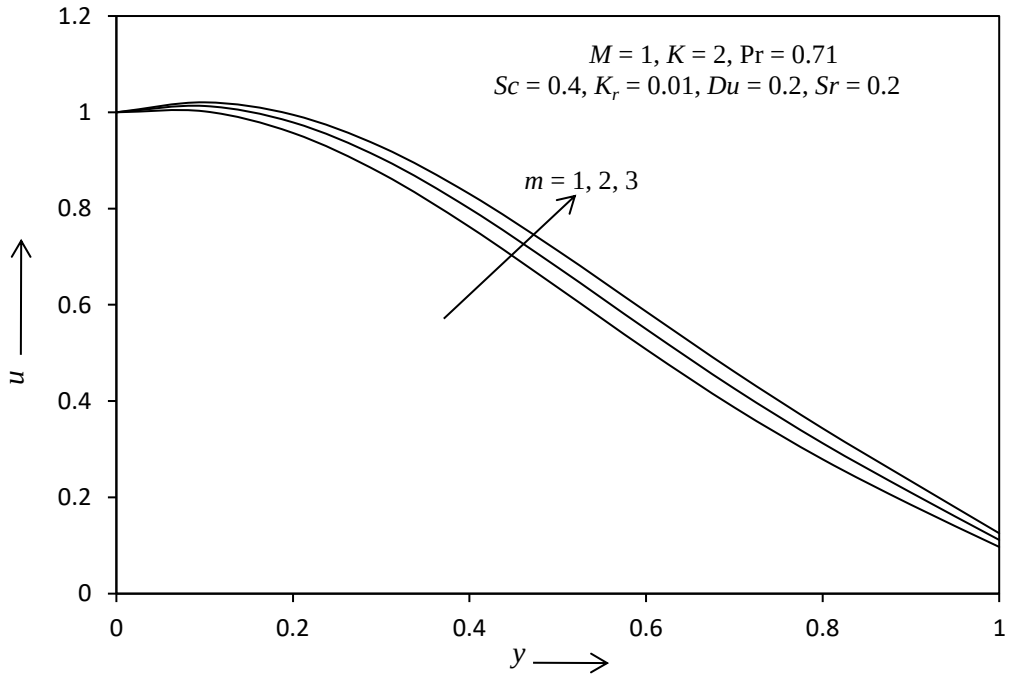

Fig. - 2: The tangential velocity profile for different value of *m*.

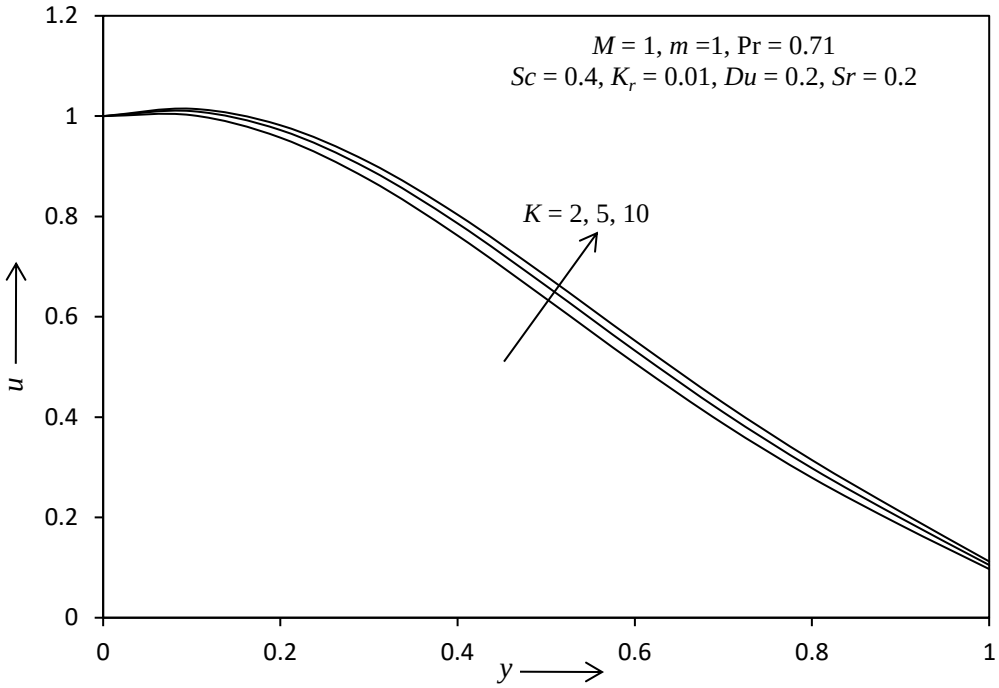

Fig. - 3: The tangential velocity profile for different value of *K*.

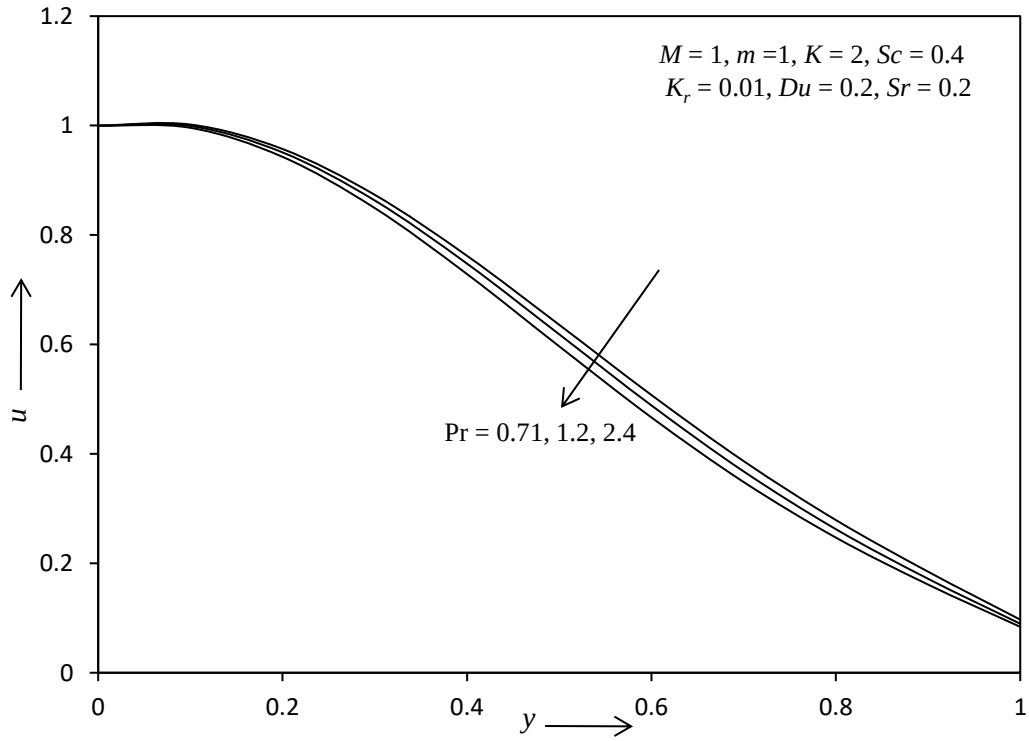

Fig. - 4: The tangential velocity profile for different value of Pr.

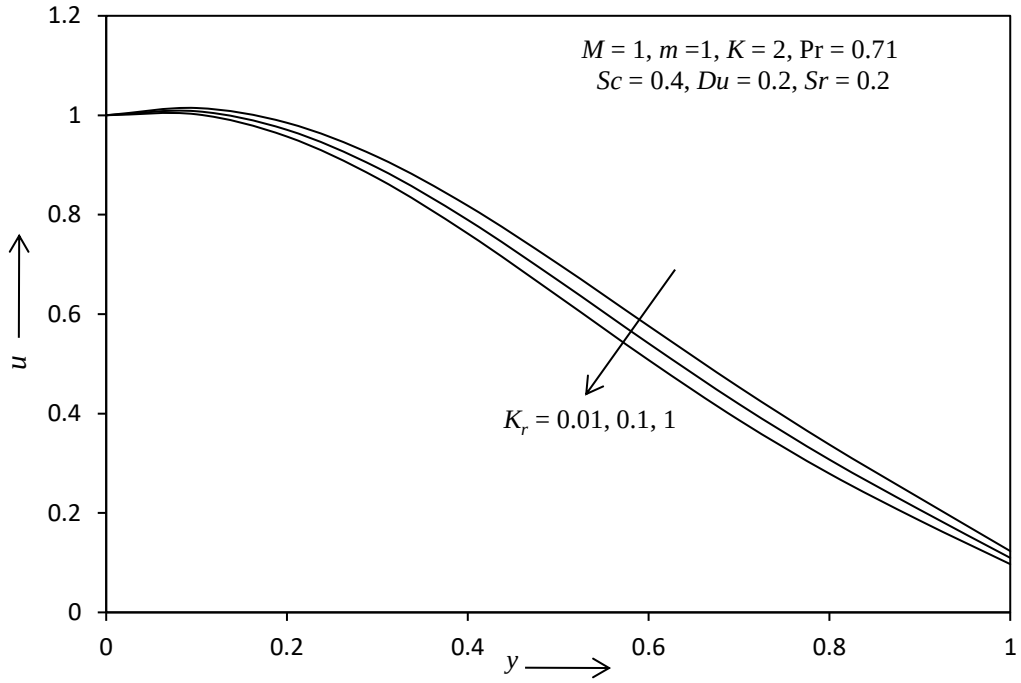

Fig. - 5: The tangential velocity profile for different value of K_r.

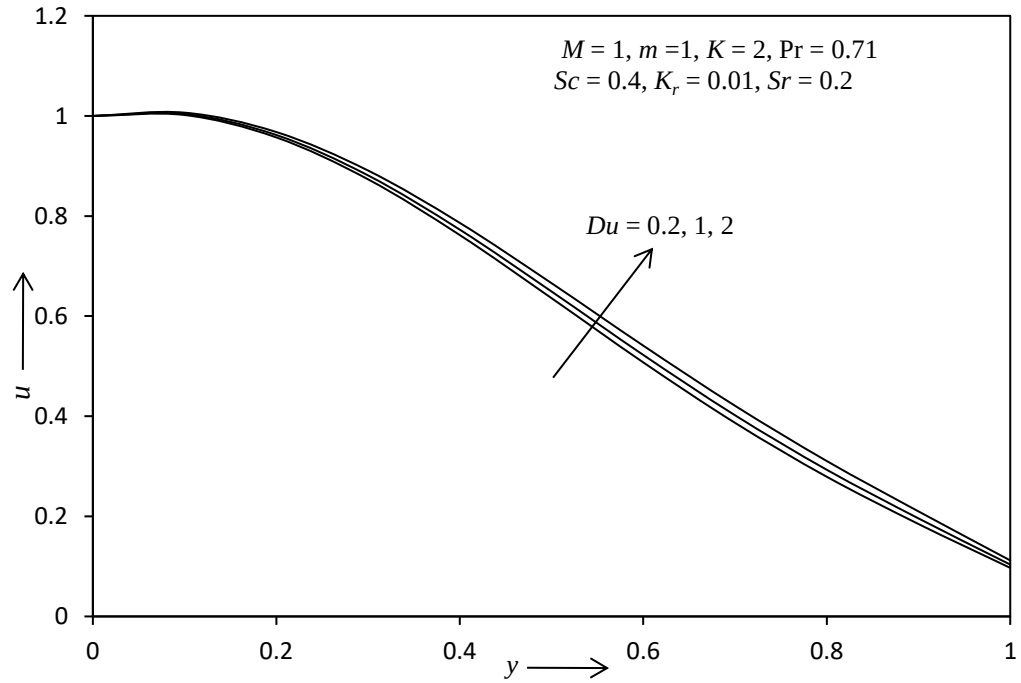

Fig. - 6: The tangential velocity profile for different value of *Du*.

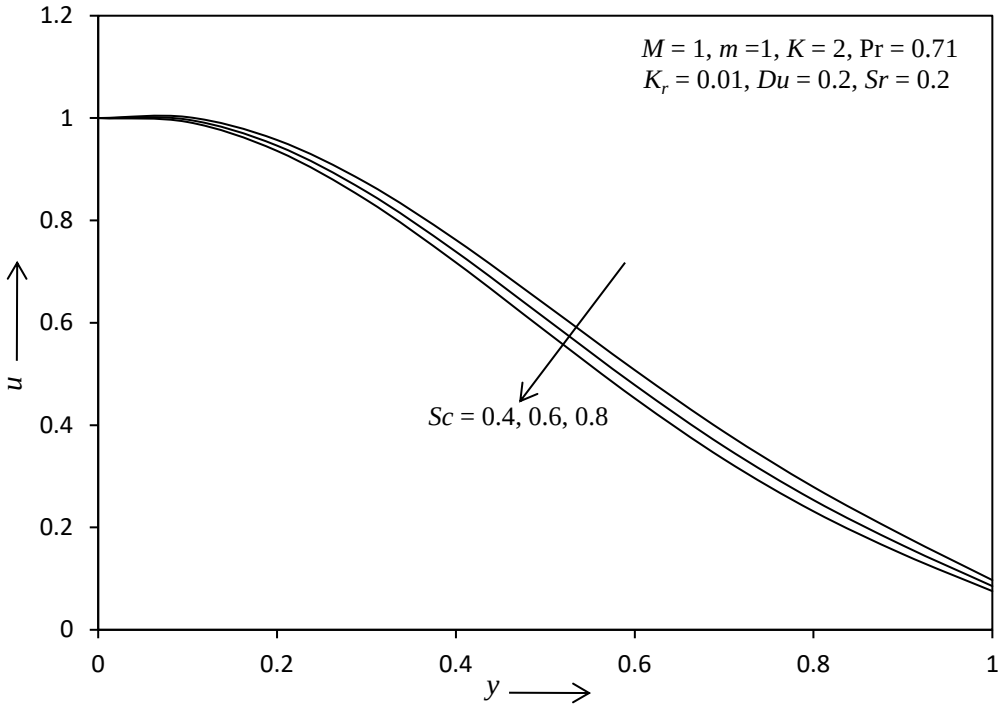

Fig. - 7: The tangential velocity profile for different value of *Sc*.

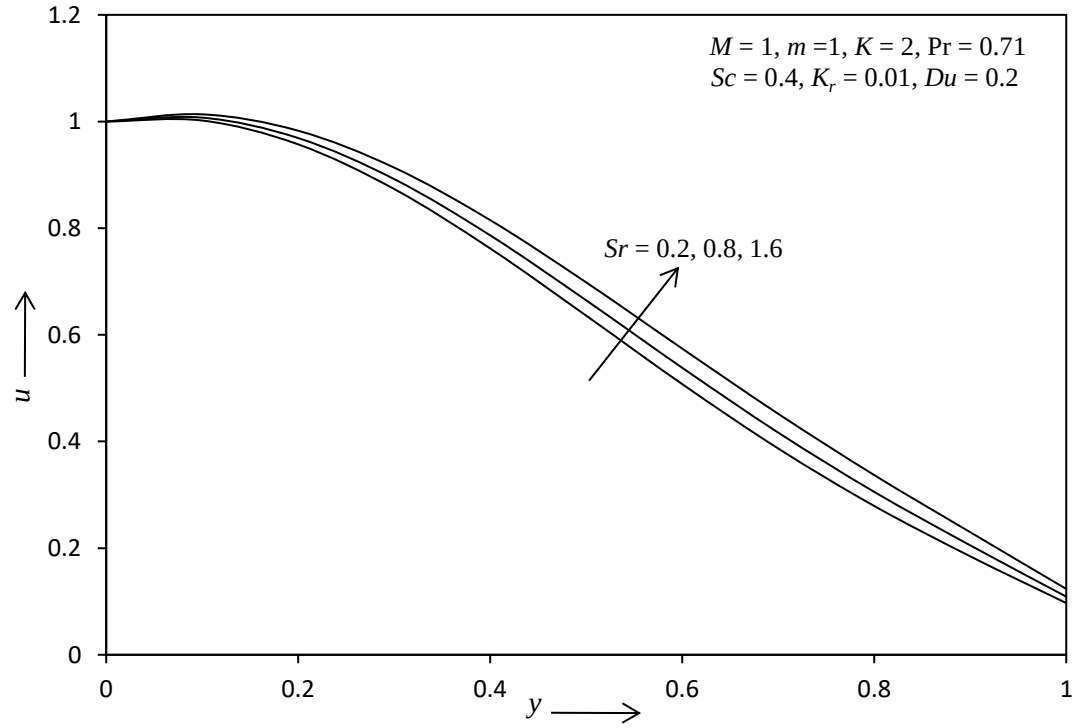

Fig. - 8: The tangential velocity profile for different value of *Sr*.

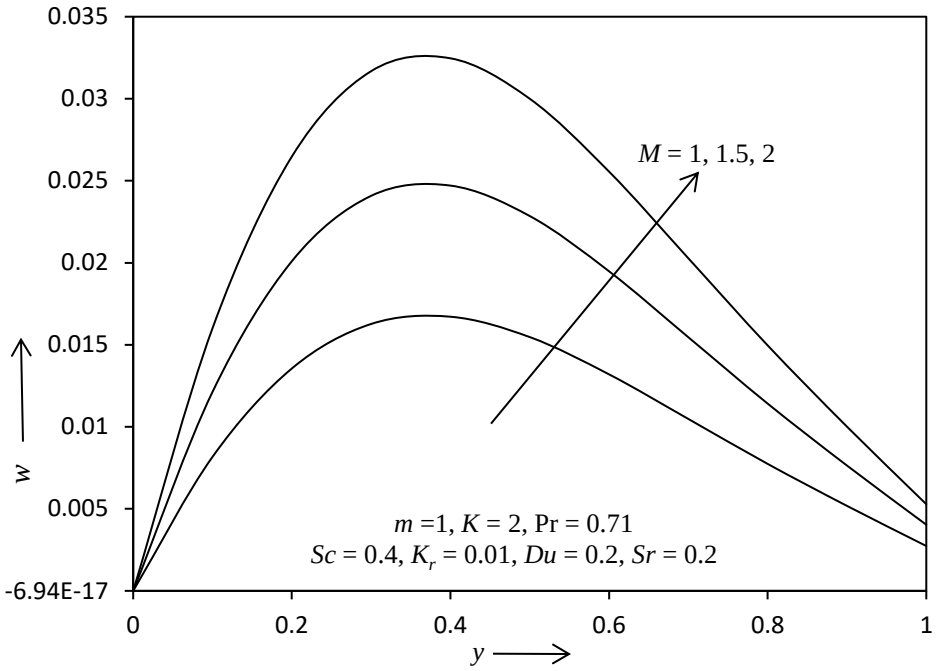

Fig. - 9: The lateral velocity profile for different value of *M*.

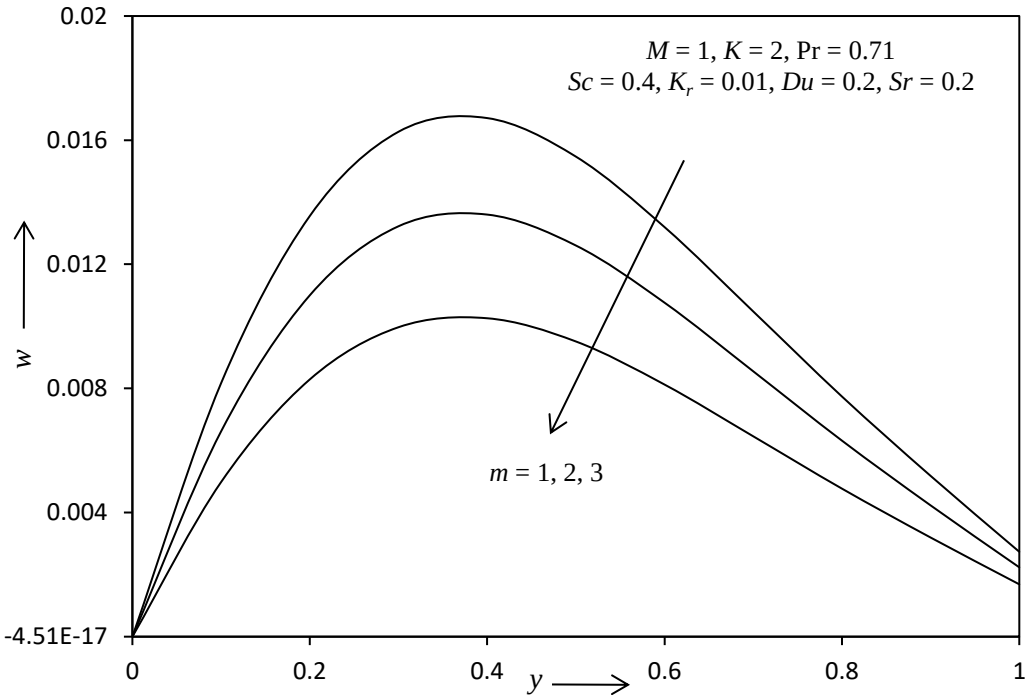

Fig. - 10: The lateral velocity profile for different value of *m*.

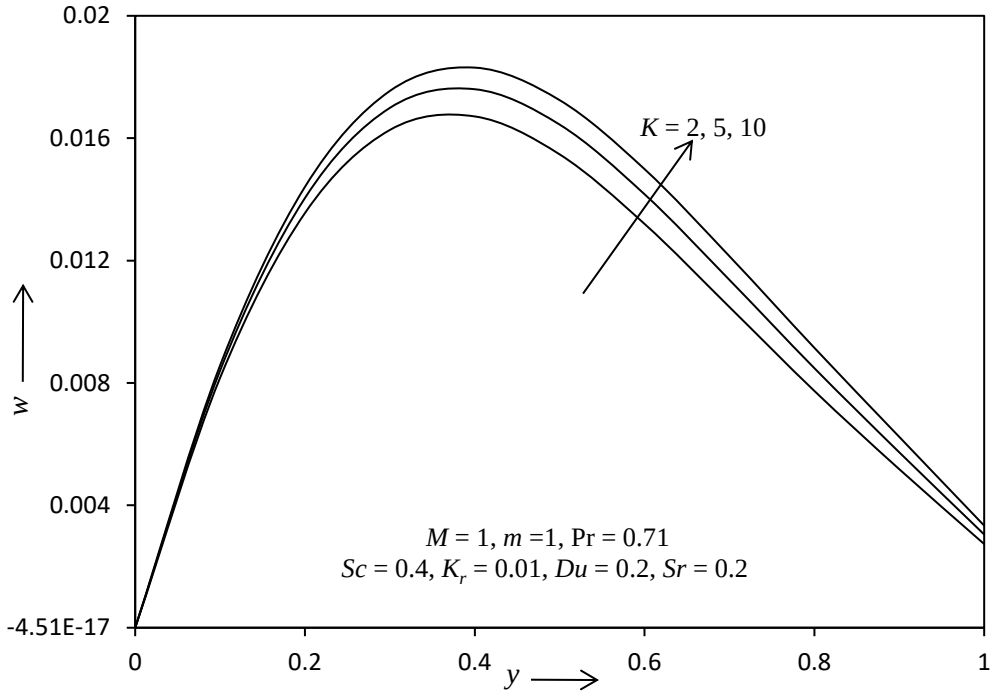

Fig. - 11: The lateral velocity profile for different value of *K*.

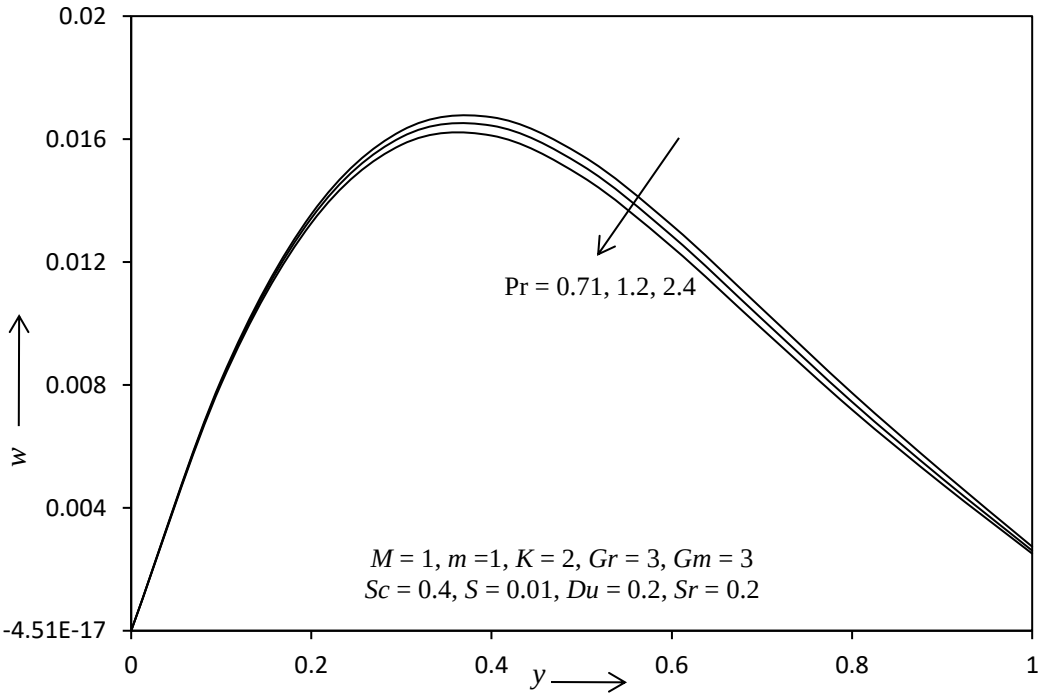

Fig. - 12: The lateral velocity profile for different value of Pr.

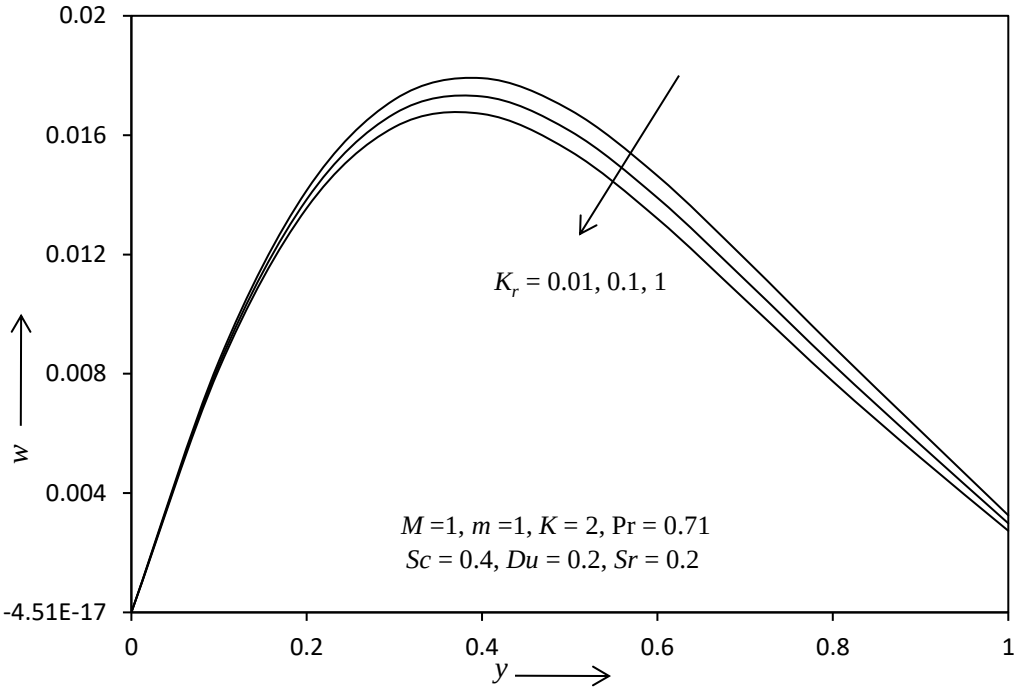

Fig. - 13: The lateral velocity profile for different value of K_r.

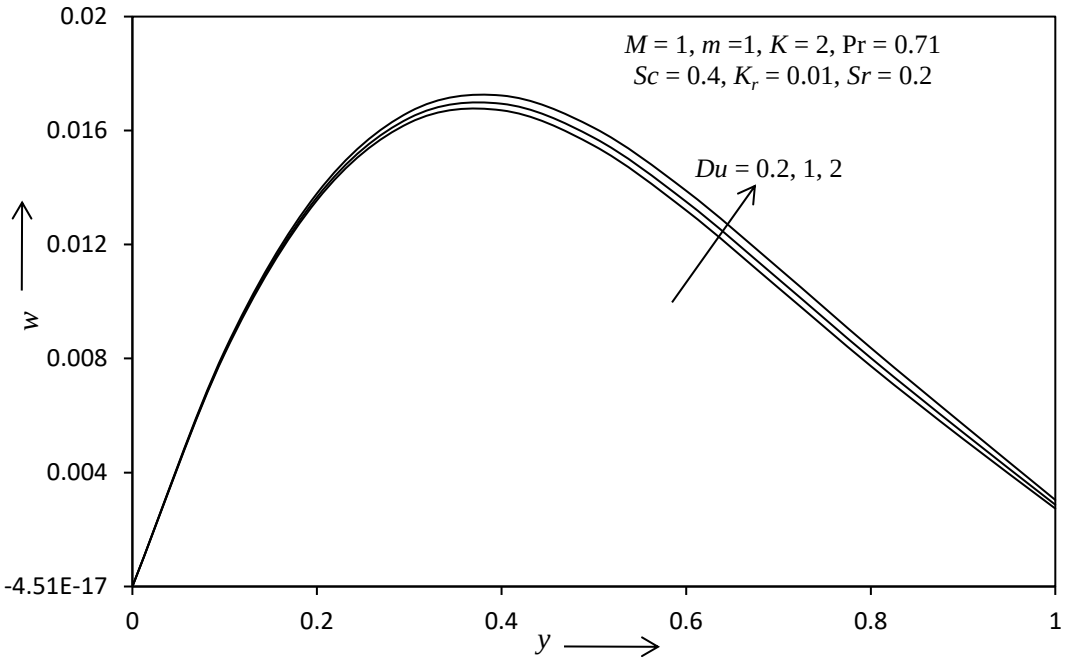

Fig. - 14: The lateral velocity profile for different value of *Du*.

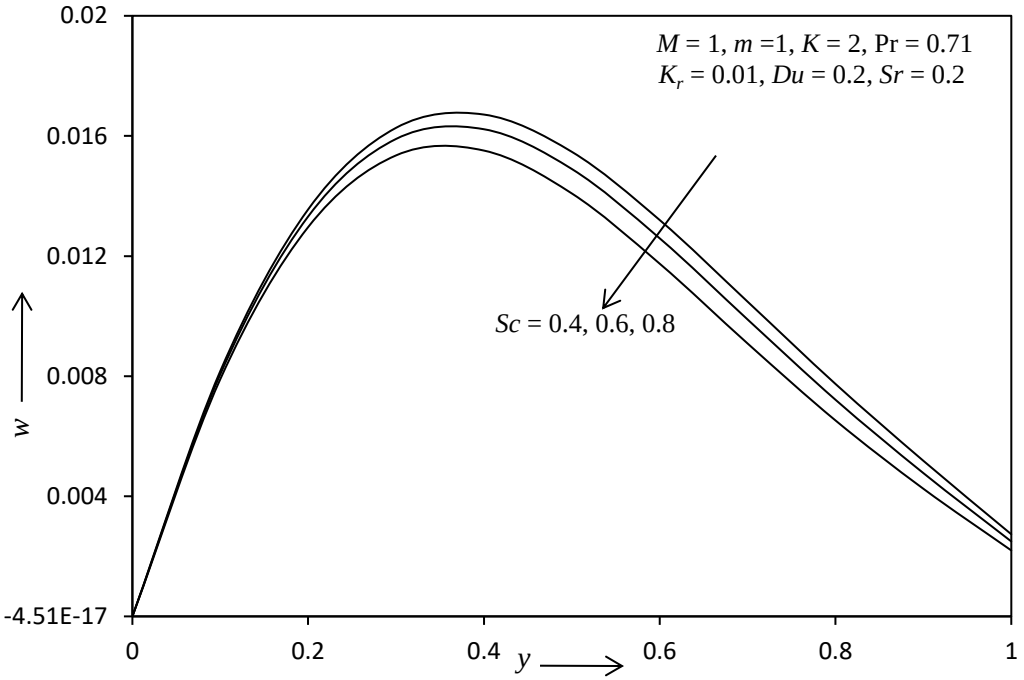

Fig. - 15: The lateral velocity profile for different value of *Sc*.

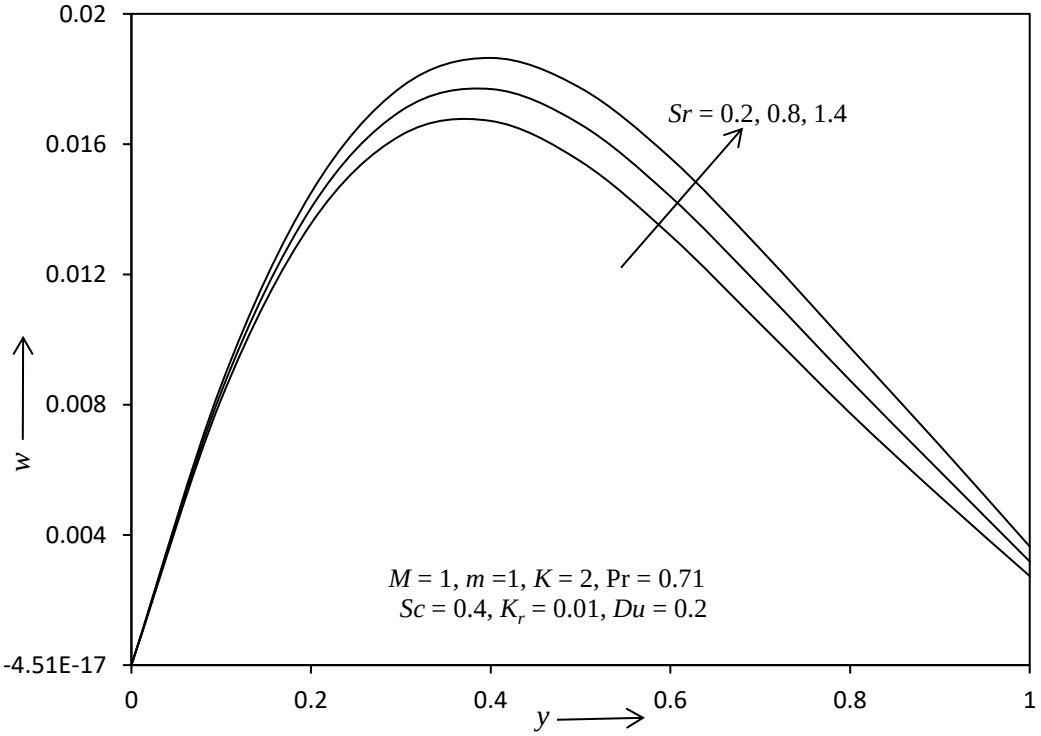

Fig. - 16: The lateral velocity profile for different value of *Sr*.

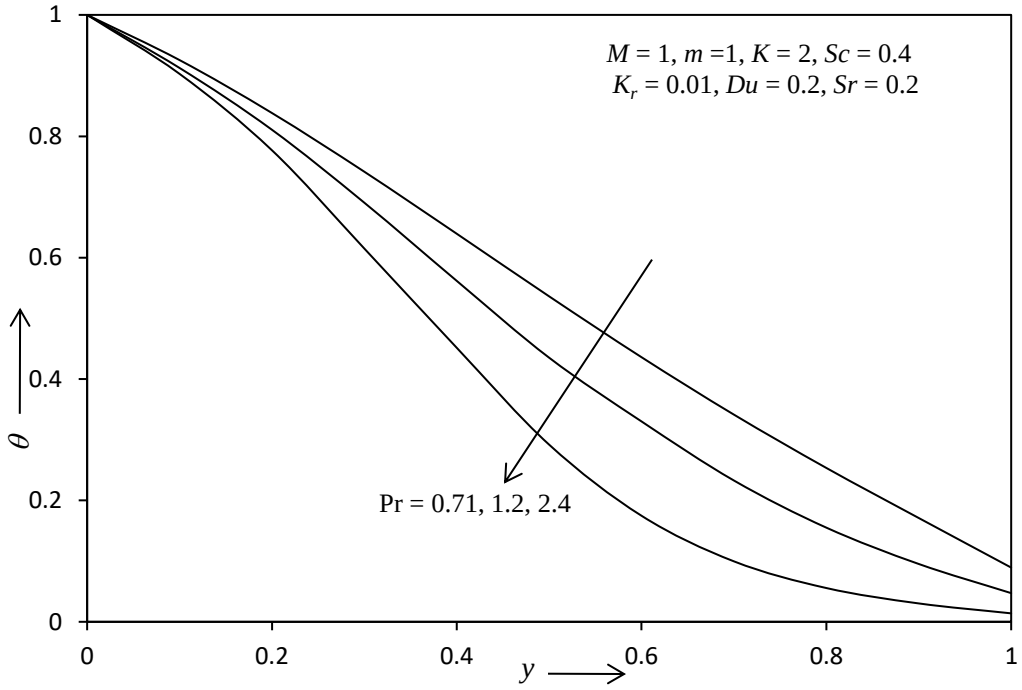

Fig. - 17: The temperature profile for different value of Pr.

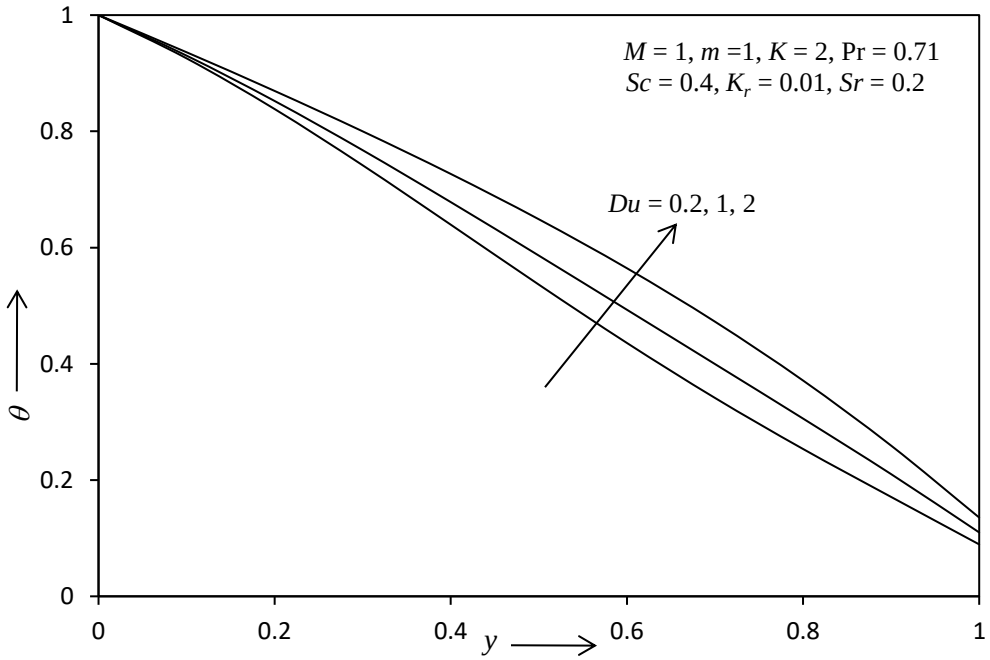

Fig. - 18: The temperature profile for different value of *Du*.

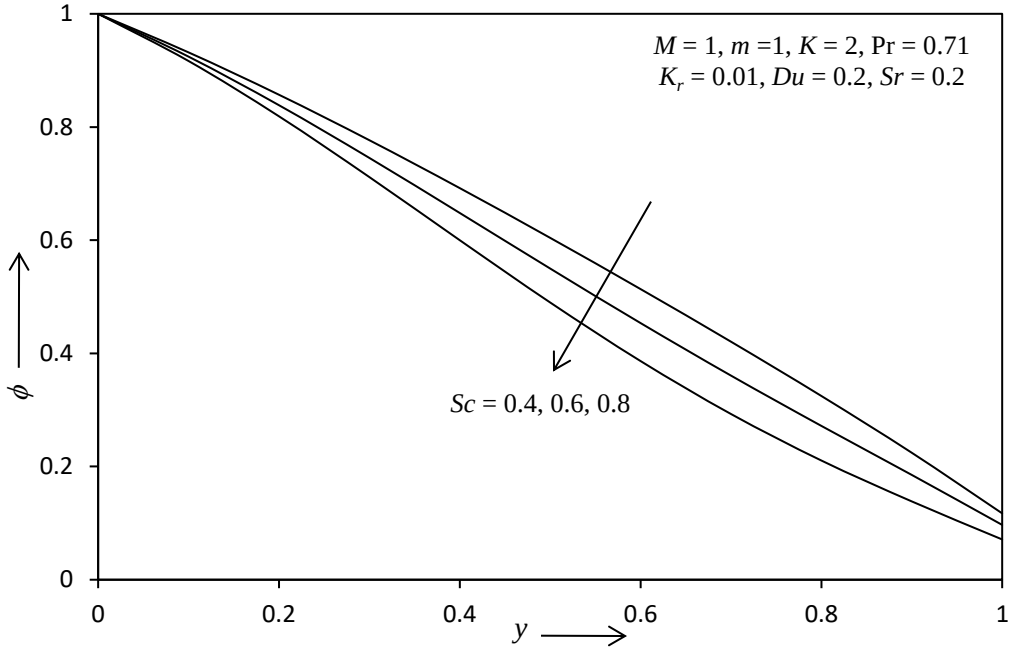

Fig. - 19: The concentration profile for different value of *Sc*.

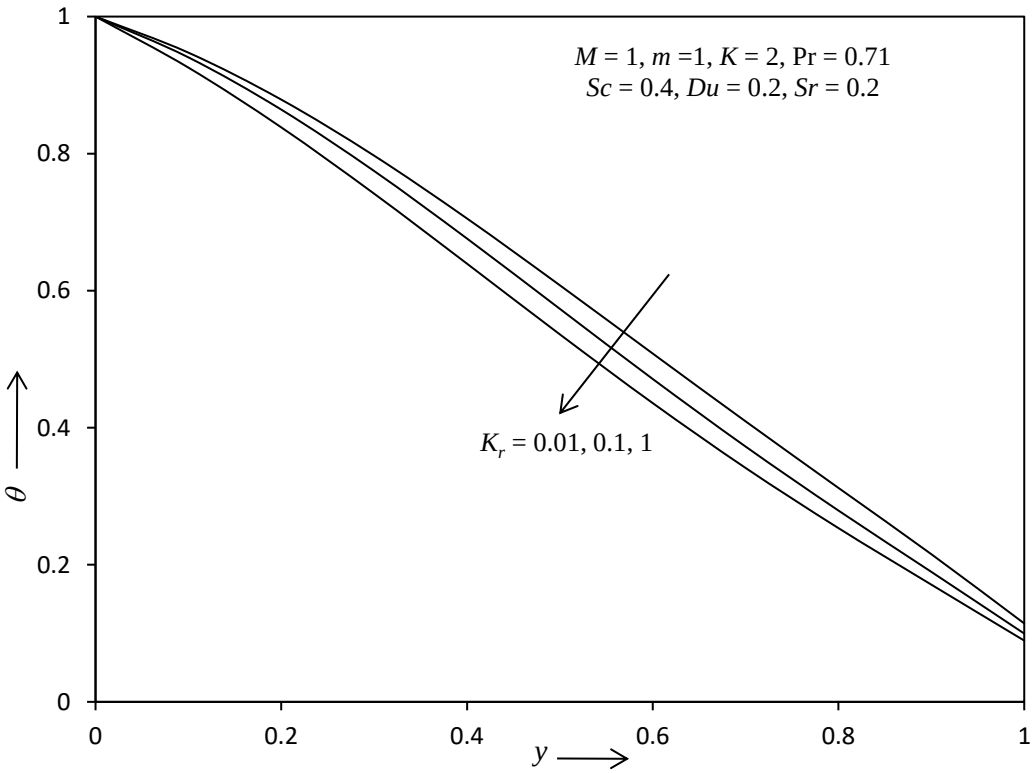

Fig. - 20: The Concentration profile for different value of K_r.

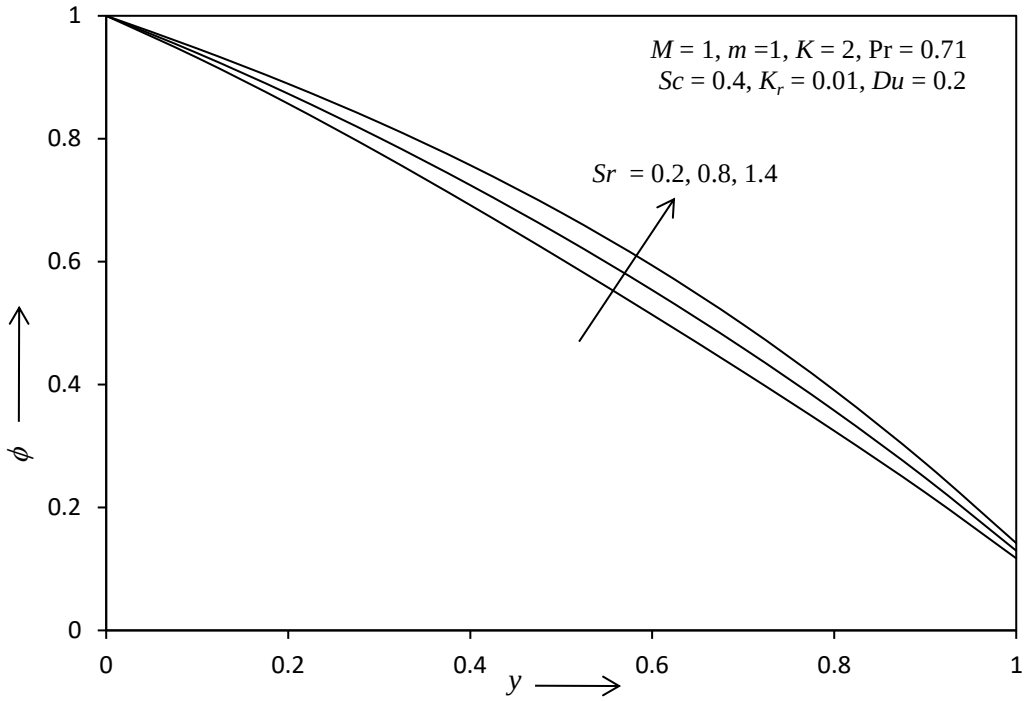

Fig. - 21: The concentration profile for different value of *Sr*.

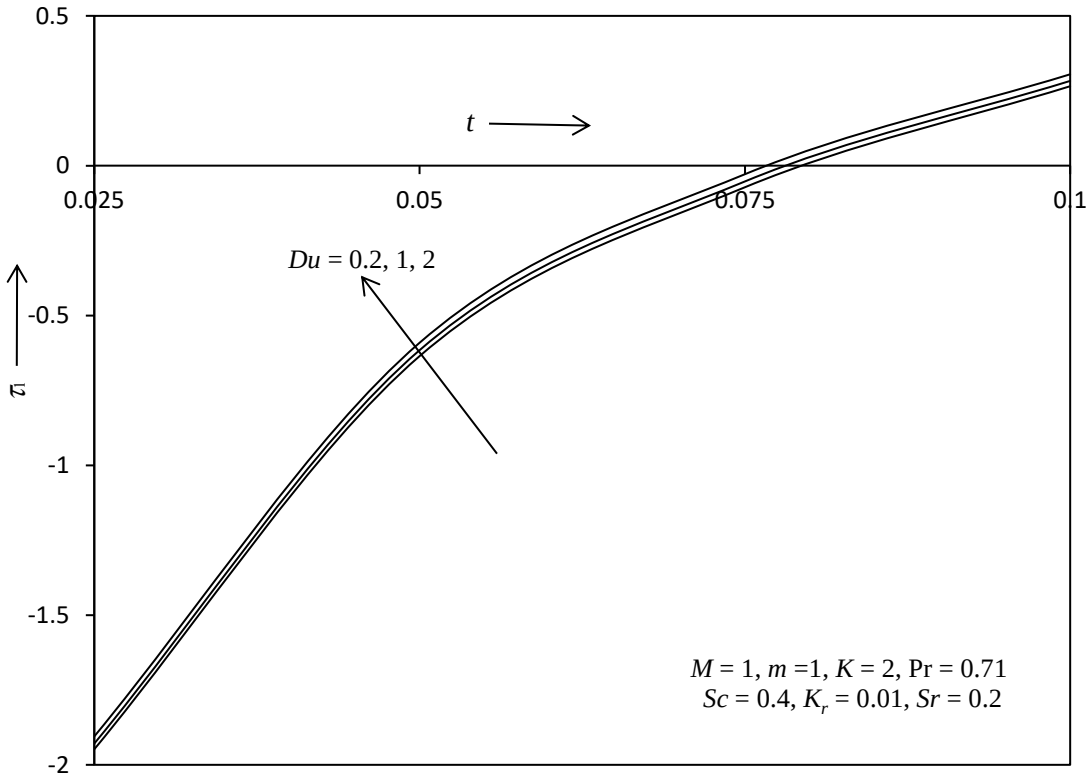

Fig. - 22: The skin friction of tangential velocity for different value of *Du*.

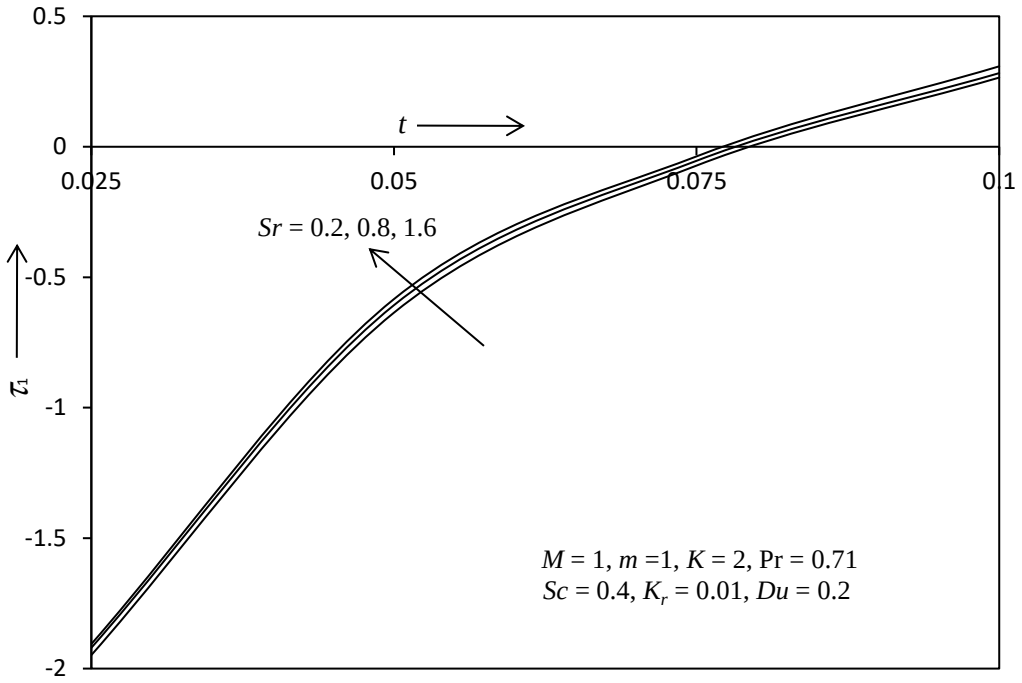

Fig. - 23: The skin friction of tangential velocity for different value of *Sr*.

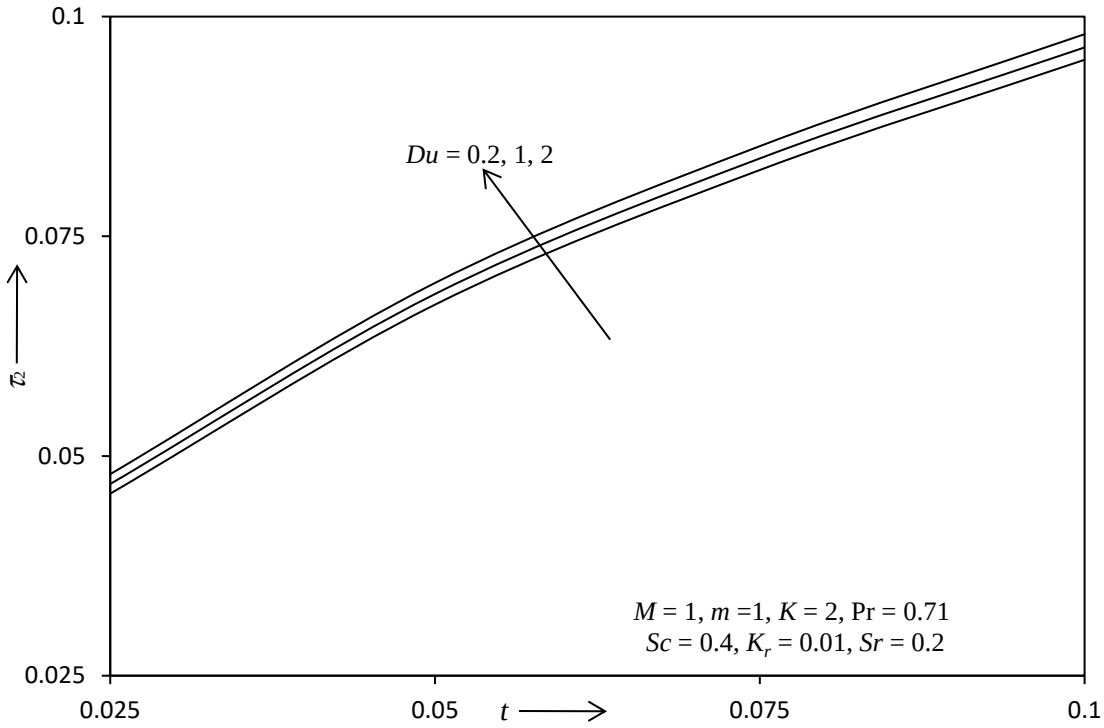

Fig.- 24: The skin friction of lateral velocity for different value *Du*.

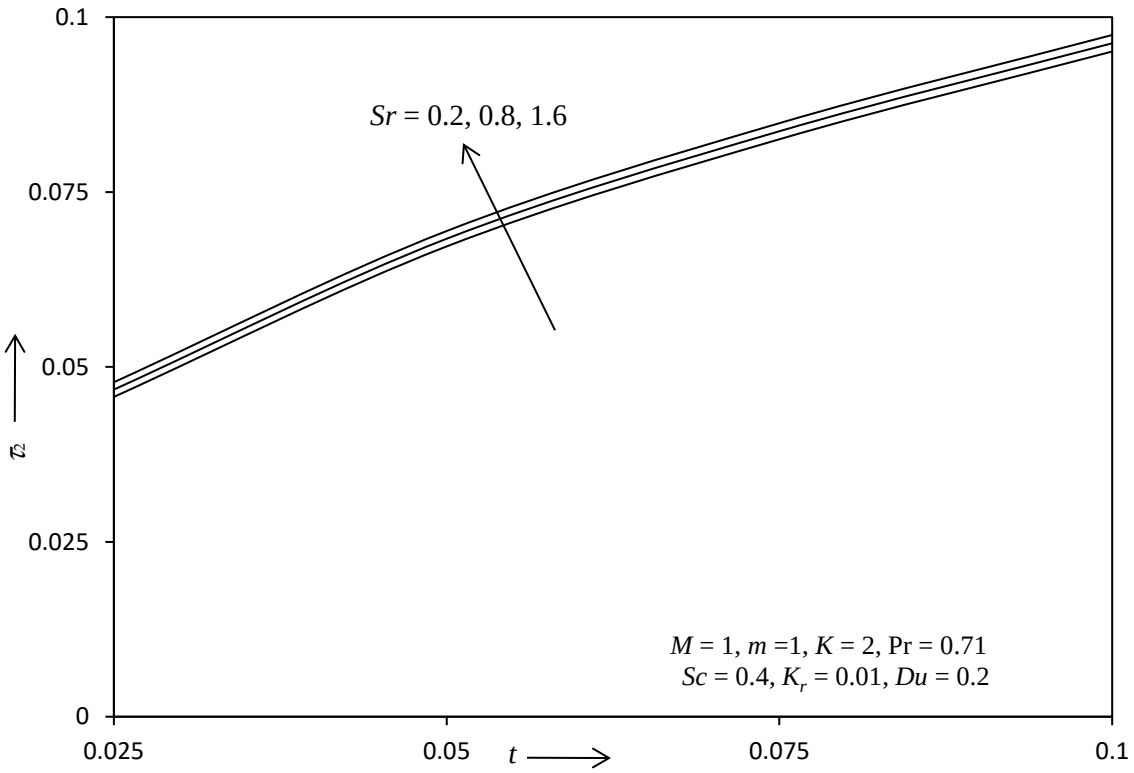

Fig.- 25: The skin friction of lateral velocity for different value *Du*.